Synthesis and mesomorphic properties of chiral liquid crystals derived from (*S*)-lactic acid with 3-pentanol

S. -L. Wu; C. -Y. Lin

PLEASE SCROLL DOWN FOR ARTICLE

Synthesis and mesomorphic properties of chiral liquid crystals derived from (*S*)-lactic acid with 3-pentanol

S.-L. WU* and C.-Y. LIN

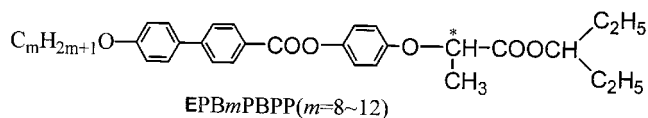Department of Chemical Engineering, Tatung University, 40 Chungshan N. Rd., 3rd Sec., Taipei, 104, Taiwan, ROC

The chiral swallow-tailed liquid crystals, 1-ethylpropyl (*R*)-2-[4-(4′-alkoxybiphenylcarbonyloxy)-phenoxy]propionates, EP*m*PBPP (*m* = 8–12), were prepared by using chiral (*S*)-lactic acid with 3-pentanol as starting materials. Mesophases and their corresponding transition temperatures were determined by polarizing microscopic textures and DSC. The results showed that all the chiral materials exhibited enantiotropic BP, N*, TGB$_A^*$, SmA*, and SmC* phases. Spontaneous polarization, dielectric constant and electro-optical response for the materials in the ferroelectric SmC* phase were investigated. It was noted that the electro-optical response of transmittance versus applied voltage obtained from the ferroelectric phase of material EP*m*PBPP (*m* = 10) displayed V-shaped switching, while that of other materials displayed the typical characteristics of ferroelectric hysteresis switching or U-shaped switching.

1. Introduction

Achiral materials with swallow-tailed moieties have been demonstrated to possess a SmC$_{alt}$ phase with antiferroelectric-like structure [1, 2]. The chiral material, (*S*)-EP10PBNP, derived from optically active (2*S*)-2-(6-hydroxy-2-naphthyl)propionic acid with 2-ethyl-propanol as a swallow-tailed group has been shown to possess antiferroelectricity [3]. Moreover, the electro-optical response of transmittance versus applied voltage in the antiferroelectric phase of this material displayed a thresholdless, V-shaped switching property. V-shaped switching was first found and reported by Inui *et al.* [4] in a mixture of antiferroelectric liquid crystals. This type of antiferroelectric mixture has been studied extensively [5–10] due to the promising potential for display devices [11].

In this work, we designed a new series of chiral swallow-tailed materials derived from the chiral moiety that is prepared by reacting optically active (*S*)-lactic acid with 2-ethylpropanol. (*S*)-Lactic acid is a commercial available chiral compound and has been widely used as a chiral moiety for the preparation of chiral liquid crystals [12–17]. The general structural formula for the target compounds is depicted below.

$$C_mH_{2m+1}O-\!\!\!\bigcirc\!\!\!-\!\!\!\bigcirc\!\!\!-COO-\!\!\!\bigcirc\!\!\!-O-\overset{*}{C}H-COOCH\begin{matrix}C_2H_5\\C_2H_5\end{matrix}$$
$$|$$
$$CH_3$$

EPB*m*PBPP(*m*=8~12)

*Author for correspondence; e-mail: slwu@ttu.edu.tw

2. Experimental

2.1. *Characterization*

The chemical structures for intermediates and target materials were analysed by nuclear magnetic resonance spectroscopy using a Jeol EX-400 FT NMR spectrometer. Purity was checked by thin layer chromatography and further confirmed by elemental analysis using a Perkin-Elmer 2400 spectrometer. Transition temperatures and phase transition enthalpies of compounds were determined by differential scanning calorimetry (DSC) using a Perkin-Elmer DSC7 calorimeter at running rates from 1 to $20°C\ min^{-1}$. Mesophases were principally identified by microscopic texture of the materials between two glass plates under crossed polarizers using a Nikon MICROPHOT-FXA in conjunction with an Instec HS1 hot stage.

The physical properties of the ferroelectric phase for the materials were measured in homogeneously aligned cells purchased from E. H. C. Co. Japan. The spontaneous polarization (P_s) was measured by a triangular wave method [18]. A triangular wave was applied to the sample from a Yogaw AG1200 arbitrary waveform generator. The induced current was displayed by measuring the voltage across a wire-wound resistor using a Hewlet-Packard HP54502A digital storage oscilloscope.

The measurement of optical transmittance versus applied electric field was made by using a He-Ne laser (5 mW, 632.8 nm) as a probe beam [19, 20]. The optical transmittance of the probe beam passing though the

cell between crossed polarizers, whose axes were parallel and perpendicular to the smectic layer normal, was detected by a photodiode. The signals were monitored by the digital oscilloscope (HP54502A). The voltage applied to the cell was produced by the arbitrary waveform generator (AG1200) and amplified by a homemade power preamplifier.

2.2. Synthesis

The target materials were prepared according to the synthetic procedure described in the scheme. 2-Ethylpropyl (S)-lactate **1** was prepared by reacting (S)-lactic acid with 3-propanol in dry benzene. 4-Hydroxyphenyl 4'-alkoxybiphenyl-4-carboxylates **2(m)** were obtained by reacting hydroquinone with 4'-alkoxybiphenyl-4-carboxylic acid chlorides, which were prepared previously by the treatment of 4'-alkoxybiphenyl-4-carboxylic acid with oxalyl chloride. The lactate **1** was then treated with the 4-hydroxyphenyl 4'-alkoxybiphenyl-4-carboxylates **2(m)** by the Mitsunobu method [21], which gave an inversion reaction in the configuration of the molecule, using diethyl azodicarboxylate (DEAD) to obtain the target materials. Detailed synthetic procedures are described below.

2.2.1. 2-Ethylpropyl (S)-lactate, **1**

(S)-Lactic acid (12 g, 0.13 mmol) and 2-ethylpropanol (8.8 g, 0.1 mmol) were dissolved in dry benzene (30 ml) and heated under reflux overnight using Dean-Stark trap to remove the water. After removing benzene solvent, the residue was distilled under vacuum, giving a 20% yield of compound **1** at 85°C 30 mm Hg^{-1}. Chemical shifts of compound **1** in ^{1}H NMR (400 MHz, CDCl₃):


Scheme.

δ (ppm) 0.76–0.84 (m, 6H), 1.31–1.36 (d, 3H), 1.38–1.55 (m, 4H), 3.84 (s, 1H), 4.21–4.15 (m, 1H), 4.76–4.70 (m, 1H).

2.2.2. 4-Hydroxyphenyl 4'-alkoxybiphenyl-4-carboxylates, **2** (m = 8–12)

4'-Alkoxybiphenyl-4-carboxylic acids (5 mmol) were treated with oxalyl chloride (12.6 mmol) in dry dichloromethane (15 ml) and heated under reflux for 2 h. The reaction mixture was then distilled under atmospheric pressure until the excess of oxalyl chloride was completely removed. The precipitates were dissolved in dry dichloromethane and added dropwise to a mixture of hydroquinone (25 mmol), dry pyridine (5 ml) and tetrahydrofuran (THF, 30 ml). After cooling the reaction mixture in a refrigerator for 2 days, silica gel was added; the mixture was then dried and powdered. The product was collected by column chromatography over silica gel (70–230 mesh) using dichloromethane as eluent. After recrystalization from ethanol, 40–50% yield of compounds **2(m)** were obtained. The results of chemical shifts, for an example of compound **2(m = 10)**, in ^{1}H NMR (400 MHz, CDCl₃): δ (ppm) 0.84–1.64 (m, 28H), 1.78–1.81 (m, 4H), 3.98–4.01 (t, 2H), 4.80–4.86 (m, 1H), 5.27–5.33 (q, 1H), 6.98–8.22 (d, d, 12H).

2.2.3. 1-Ethylpropyl (R)-2-[4-(4'-alkoxybiphenyl-carbonyloxy)phenoxy] propionates, EPmPBPP (m = 8–12)

A solution of diethyl azodicarboxylate (1.6 mmol) and **2(m)** (1.08 mmol) in 7 ml anhydrous THF was added dropwise to a solution of triphenylphosphine (Ph₃P, 1.6 mmol) and compound **1** (1.6 mmol) in 7 ml anhydrous THF at room temperature with vigorous stirring. The reaction soon started. After standing overnight at room temperature, triphenyl phosphine oxide was removed from the mixture by filtration. After a work-up procedure, the products were isolated by column chromatography over silica gel (70–230 mesh) using ethyl acetate/hexane (1/11) as eluent, and recrystallized from absolute ethanol; 40–50% yields of final product were obtained. The results of elemental analysis, as an example, of compound EPmPBPP (m = 10): calculated for C₃₇H₄₈O₆, C 75.51, H 8.16; found C 75.37, H 8.10%. Chemical shifts of EPmPBPP (m = 10) in ^{1}H NMR (400 MHz, CDCl₃): δ (ppm) 0.73–1.64 (m, 28H), 1.79 (d, 4H), 3.98–4.01 (t, 2H), 4.72–4.74 (m, 1H), 4.76 (q, 1H), 6.90–8.20 (d, d, 12H).
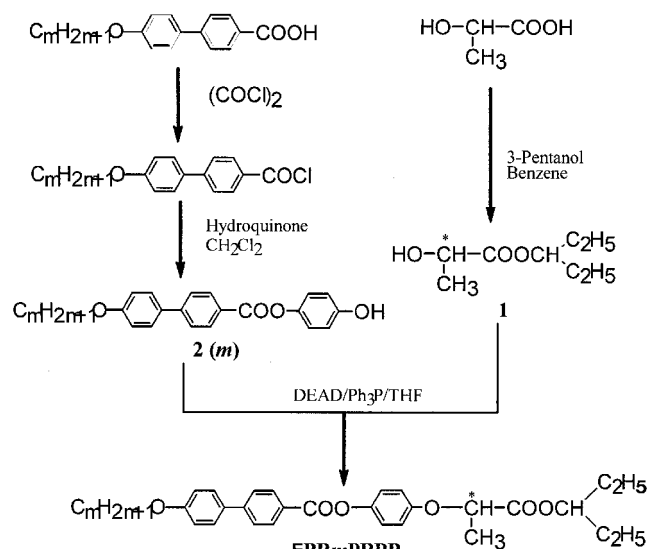
3. Results and discussion

The mesophases and their corresponding phase transition temperatures for the chiral materials were determined by texture observation using polarizing optical

microcopy (POM) and differential scanning calorimetry (DSC), respectively. All compounds exhibit enantiotropic BP, N*, TGB$_A^*$ and SmA* phases. Compounds EPmPBPP ($m = 10, 11$) display an enantiotropic SmC* phase, while the other compounds display a monotropic SmC* phase. Detailed data of phase transition temperatures and corresponding enthalpies of the transition are shown in the table.

The physical properties for the compounds were measured in 5 μm homogeneously aligned cells. Figure 1 illustrates the switching current behaviour of EPBmPBPP ($m = 10$) in the SmC* phase; one significant peak appeared, indicating the existence of a ferroelectric phase. The strength of the current peaks increase slightly with decreasing temperature, but the relative position of the peaks is almost unchanged. Figure 2 shows some representative results of spontaneous polarization **P**s
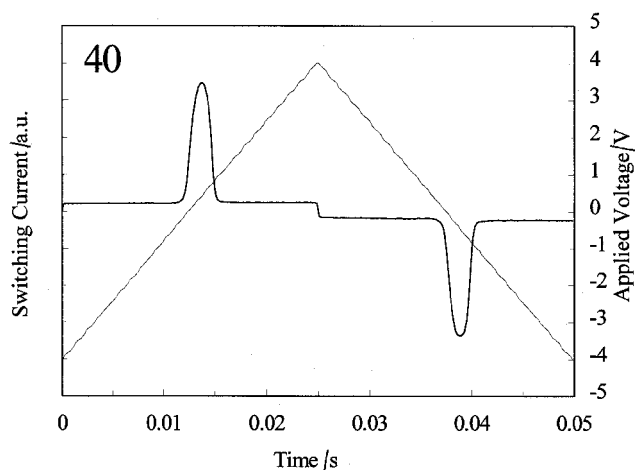

Figure 2. Spontaneous polarization plotted as a function of temperature for EPBmPBPP ($m = 9$–11). □, $m = 9$; ○, $m = 10$; ◆, $m = 11$.

Figure 1. Switching current behaviour of EPBmPBPP ($m = 10$) in the SmC* phase at 40°C in a homogeneously aligned cell of 5 μm thickness.

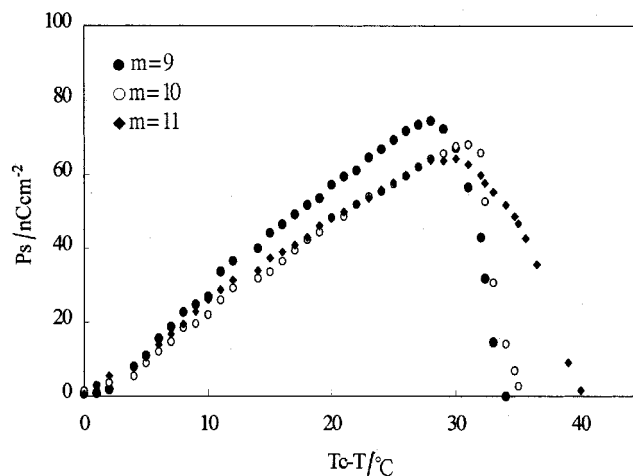as a function of temperature measured for the three materials EPBmPBPP ($m = 9$–11). The maximum **P**s values were in the range 65–75 nC cm^{-1}.

The temperature dependence of the dielectric constant ε' was measured at 100 Hz and 1 kHz in 25 μm homogeneously cells, aligned with results depicted in figure 3. During cooling, the ε' in the SmA* phase is small, increasing slightly at the SmA* to SmC* transition. The characteristic point corresponding to the SmA*–SmC* transition is easily seen in the figure. The great enhancement of the dielectric constant on cooling from SmA* to SmC* is due to the contribution of the Goldstone mode [22]. During heating, however, because the existence range of the SmC* phase is rather small (0.55°C as measured by DSC), the dielectric constant measurement indicated that the cell sample may remain as crystal, thus no dielectric constant was detected.

Table. Transition temperatures (°C) and associated enthalpy data (kJ mol^{-1}) for the chiral materials EPBmPBPP ($m = 8$–12).

m	I		BP		N*		TGB$_A^*$		SmA*		SmC*		Cr	m.p.[c]
8	•	121.2 (1.68)	•	120.5[a]	•	114.3[a]	•	112.7 (1.46)	•	65.0[b]	•	29.1 (16.04)	•	81.8 (34.92)
9	•	116.0 (1.47)	•	115.0[a]	•	110.4[a]	•	107.9 (0.99)	•	62.8[b]	•	29.3 (19.83)	•	67.2 (59.99)
10	•	114.2 (0.75)	•	113.3[a]	•	109.6[a]	•	107.8 (0.85)	•	61.0[b]	•	27.47 (37.42)	•	59.45 (51.77)
11	•	111.4 (0.43)	•	110.5[a]	•	108.6[a]	•	106.8 (0.47)	•	65.7[b]	•	32.9 (49.90)	•	64.58 (63.57)
12	•	109.9 (0.03)	•	108.6[a]	•	107.7[a]	•	105.9 (0.35)	•	65.7[b]	•	34.8 (59.2)	•	71.05 (72.34)

[a] The enthalpies of BP–N* or TGB$_A^*$–SmA* transitions were added together with that of the I–BP or N*–TGB$_A^*$ transition.
[b] The enthalpy was too small to be measured.
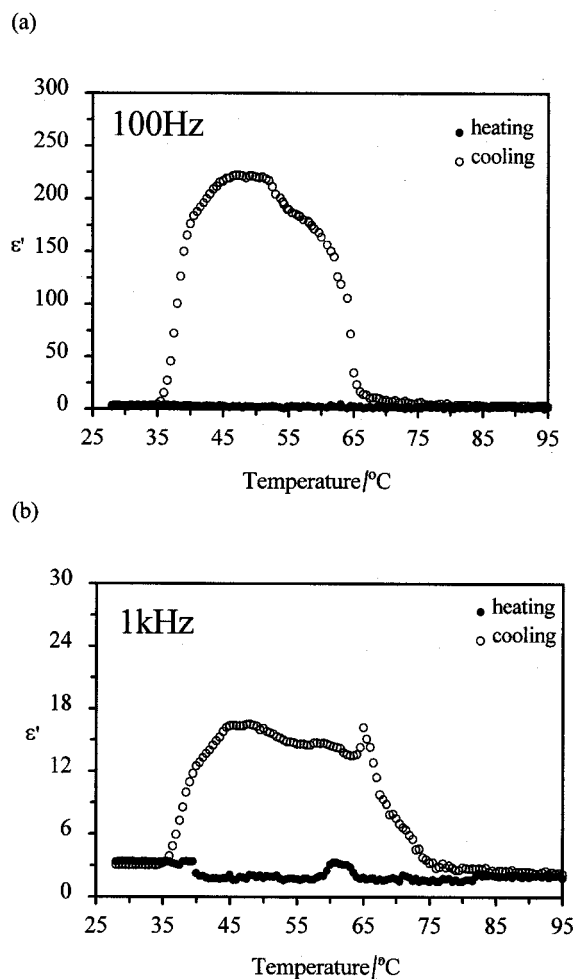[c] mp. refers to the melting point taken from DSC thermograms, recorded at heating rates of 2°C min^{-1}.

(a)

(b)

Figure 3. Temperature dependence of the real part of the dielectric constant for EPB*m*PBPP (*m* = 10) at (*a*) 100 Hz (*b*) 1 kHz.

Electrical Field / V/ μ m

Figure 4. Transmittance versus electrical field obtained in the SmC* phase of compound EPB*m*PBPP (*m* = 10) at several temperatures on applying a triangular wave.

Electro-optical responses were obtained under crossed polarizers where the axes of polarizer and analyser were parallel and perpendicular, respectively, to the smectic layer normal in 5 µm homogeneously aligned cells. Figure 4 illustrates the variation of transmittance with electric field on application of triangular waveform field measured in the SmC* phase for compound EPB*m*PBPP (*m* = 10). The responses are critically depended on temperature and frequency. As the temperature decreases, the maximum transmittance values increase due to the increase of the tilt angle [8]. At 5 Hz, the curves of transmittance versus applied field display a W-shaped feature in the SmC* phase. Furthermore, as the frequency decreases from 5 to 1 Hz, the W-shaped switching evolves into V-shaped switching, as shown in figure 4 at 50°C and 45°C under 1 Hz of applied frequency. However, it was found that the darkest state at the tip of the V in V-shaped switching is not located at zero
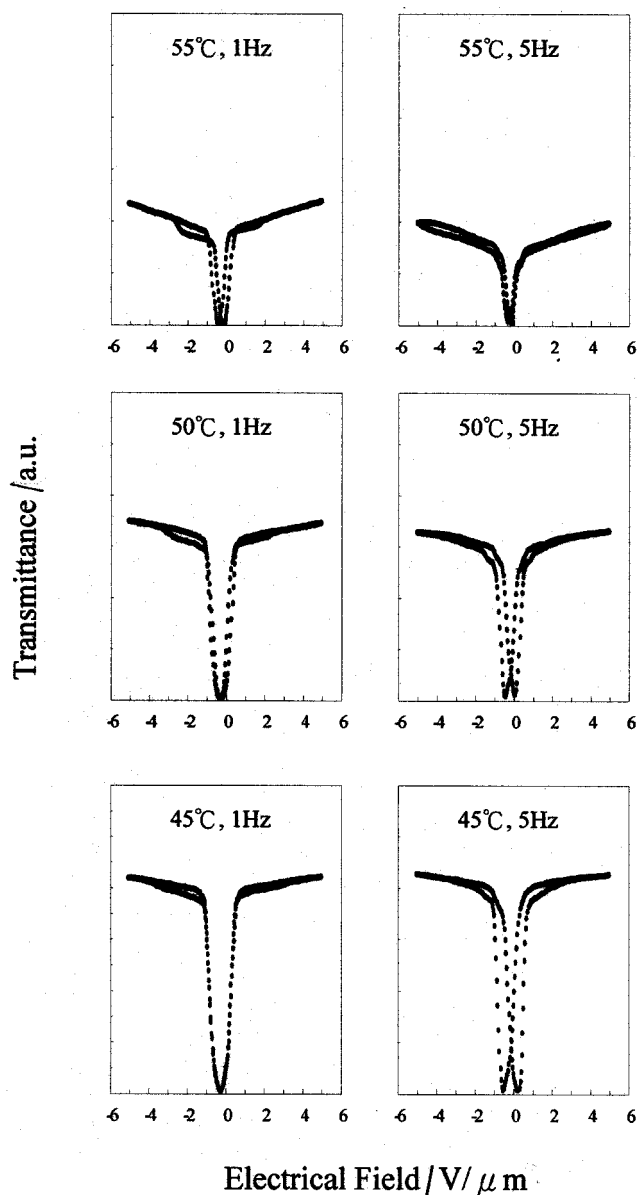
field. This switching behaviour has also been observed by Chandani *et al.* [9], who explained that interaction between the liquid crystal molecules and the alignment layer could dominate, giving rise to the laterally shifted V-shaped switching.

The electro-optical responses for the other materials were also determined, to investigate the effect of the non-chiral peripheral chain. All results were similar, as shown for example, in the figure 5 for EPB*m*PBPP (*m* = 11). At 1 Hz of applied frequency, the characteristic ferroelectric hysteresis loop appeared in the higher temperature region of the SmC* phase, which is different
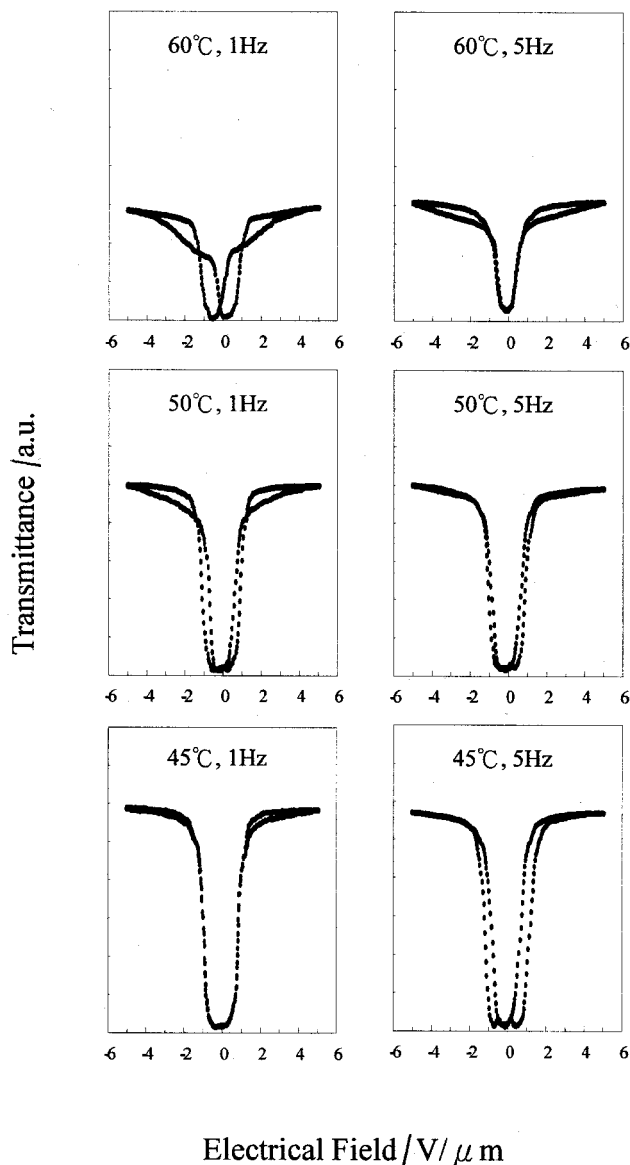
Figure 5. Transmittance versus electrical field obtained in the SmC* phase of compound EPB*m*PBPP (*m* = 11) at several temperatures on applying a triangular wave.

from that observed in EPB*m*PBPP (*m* = 10). Furthermore, the hysteresis switching altered to a hysteresis-free, U-shaped switching at lower temperatures. It is interesting to note that as the applied frequency increased from 1 to 5 Hz, an opposite trend to the switching behaviour occurred, i.e. a U-shaped switching appeared at the higher temperature region of the SmC* phase, whereas a typical ferroelectric hysteresis switching occurred in the lower temperature region. It is suggested that the switching of the electro-optical response for ferroelectric liquid crystals critically depends on the applied frequency.

4. Conclusion

Chiral swallow-tailed materials EPB*m*PBPP (*m* = 8–12) derived from (*S*)-lactic acid have been demonstrated to possess a ferroelectric SmC* phase. The electro-optical response obtained from compound EPB*m*PBPP (*m* = 10) in the ferroelectric SmC* phase displayed V-shaped switching, while that obtained from the other materials displayed a typical hysteresis loop characteristic of ferroelectric materials. It is concluded that the switching behaviour of the electro-optical response in homogeneously aligned cells depends on the molecular structure of the liquid crystal.

References

[1] Booth, C. J., Dunmur, D. A., Goodby, J. W., Haley, J., and Toyen, K. J., 1996, *Liq. Cryst.*, **20**, 387.
[2] Wu, S.-L., and Chiang, C.-T., 2002, *Liq. Cryst.*, **29**, 39.
[3] Wu, S.-L., and Hsieh, W.-J., 1999, *J. mater. Chem.*, **11**, 852.
[4] Inui, S., Iimura, N., Suzuki, T., Iwane, H., Miyachi, K., Takanishi, Y., and Fukuda, A., 1996, *J. mater. Chem.*, **6**, 71.
[5] Fukuda, A., Seomun, S. S., Takahashi, T., Takahashi, Y., and Ishikawa, K., 1997, *Mol. Cryst. liq. Cryst.*, **303**, 379.
[6] Seomun, S. S., Takahashi, Y., Ishikawa, K., Tkezoe, H., Fukuda, A., Tanaka, C., Fujiyama, T., Maruyama, T., and Nishiyama, S., 1997, *Mol. Cryst. liq. Cryst.*, **303**, 181.
[7] Seomun, S. S., Takahashi, Y., Ishikawa, K., Tkezoe, H., and Fukuda, A., 1997, *Jpn. J. appl. Phys.*, **36**, 3586.
[8] Seomun, S. S., Gouda, T., Takahashi, Y., Ishikawa, K., Ishikawa, K., Tkezoe, H., and Fukuda, A., 1999, *Liq. Cryst.*, **26**, 151.
[9] Chandani, A. D. L., Cui, Y., Seomun, S. S., Takahashi, Y., Ishikawa, K., Tkezoe, H., and Fukuda, A., 1999, *Liq. Cryst.*, **26**, 167.
[10] Chandani, A. D. L., Cui, Y., Seomun, S. S., Takahashi, Y., Ishikawa, K., Tkezoe, H., and Fukuda, A., 1998, *Mol. Cryst. liq. Cryst.*, **322**, 337.
[11] Saishu, T., Tkatoh, K., Iida, R., Nagata, H., and Mori, Y., 1996, *SID'96.*, **28**, 4.
[12] Kašpar, M., Glogarova, M., Hamplova, V., Sverenyàk, H., and Pakhomov, S. A., 1993, *Ferroelectrics*, **148**, 103.
[13] Kašpar, M., Sverenyàk, H., Hamplova, V., Glogarova, M., Pakhomov, S. A., Vanek, P., and Trunda, B., 1995, *Liq. Cryst.*, **19**, 775.
[14] Kašpar, M., Hamplova, V., Pakhomov, S. A., Stibor, I., Sverenyàk, H., Bubnov, M. A., Glogarova, M., and Vanek, P., 1997, *Liq. Cryst.*, **22**, 557.
[15] Hamplova, V., Kašpar, M., Pakhomov, S., Bubnov, A., and Glogarova, M., 1999, *Mol. Cryst. liq. Cryst.*, **322**, 181.
[16] Bubnov, A., Hamplova, V., Kašpar, M., Vanek, P., Pociecha, D., and Glogarova, M., 2001, *Mol. Cryst. liq. Cryst.*, **366**, 547.

[17] KAŠPAR, M., HAMPLOVÀ, V., NOVOTNÀ, V., GLOGAROVÀ, M., POCIECHA, D., and VANEK, P., 2001, *Liq. Cryst*., **28,** 1203.

[18] MIYASATO, K., ABE, S., TAKEZOE, H., FUKUDA, A., and KUZE, E., 1983, *Jpn. J. appl. Phys.*, **22,** L661.

[19] CHANDANI, A. D. L., HAGIWARA, T., SUZUKI, Y., OUCHI, Y., YAKAZOE, H., and FUKUDA, A., 1988, *Jpn. J. appl. Phys.*, **27,** L729.

[20] LEE, J., CHANDANI, A. D., ITOH, K., OUCHI, Y., TAKEZOE, H., and FUKUDA, A., 1990, *Jpn. J. appl. Phys.*, **29,** 1122.

[21] MISTUNOBU, O., YAMADA, M., and MUKAIYAMA, T., 1967, *Bull. chem. Soc. Jpn.*, **40,** 2380.

[22] CEPIC, M., HEPPKE, G., HOLLIDT, J. M., LOTZSCH, D., and BEKS, B., 1994, *Ferroelectrics*, **147,** 179.